UC Irvine
UC Irvine Previously Published Works

Title

Thermal expansion coefficients of rare earth metal disilicides and their influence on the growth of disilicide nanowires

Permalink

Journal

ISSN

Authors

Yang, JJ
Rawn, CJ
Ji, C-X
et al.

Publication Date

DOI

Copyright Information

Peer reviewed

J.J. YANG[1]
C.J. RAWN[2]
C.-X. JI[1]
Y.A. CHANG[1],✉
Y. CHEN[3]
R. RAGAN[3]
D.A.A. OHLBERG[3]
R.S. WILLIAMS[3]

Thermal expansion coefficients of rare earth metal disilicides and their influence on the growth of disilicide nanowires

[1] Department of Materials Science and Materials Science Program, University of Wisconsin-Madison, 1509 University Avenue, 53706 Madison, WI, USA

[2] Metals and Ceramics Division, Oak Ridge National Laboratory, 37831 Oak Ridge, TN, USA

[3] Quantum Science Research, Hewlett-Packard Laboratories, 1500 Page Mill Road, MS 1123, 94304 Palo Alto, CA, USA

ABSTRACT The lattice parameters of rare earth metal disilicides at high temperature play a crucial role in the growth of these disilicide nanowires, which takes place at about 873 K. In the present study, the lattice parameters of Sm, Gd, Tb, Dy, Ho, Er, Sc and Er_xGd_{1-x} disilicides with AlB_2 structure were measured from room temperature to about 873 K by high temperature X-ray diffraction (HTXRD), from which the linear coefficient of thermal expansion (CTE) along each crystallographic axis was determined. The influence of the CTEs on the growth of nanowires will be discussed in terms of anisotropic strain. With these CTEs, the composition of a ternary disilicide, $(Er_xGd_{1-x})Si_{1.67}$, for example, with optimal lattice parameters at nanowire growth temperature can be engineered to meet the requirement for the growth of high-quality nanowires.

PACS 65.40.De; 68.65.La; 68.55.-a

1 Introduction

The success in growing self-assembled erbium disilicide nanowires by Chen et al. [1] has motivated intense research activities on the formation of rare earth metal disilicide nanowires. Experimentally, disilicide nanowires have been grown on Si(001) substrates by evaporating rare earth metals, such as Gd, Ho, Sm, Dy, and Sc [2–10]. Theoretical models have also been proposed to understand the formation of these nanowires [11–13]. The [0001] axis of the disilicide nanowire is oriented along a ⟨110⟩ axis of the Si(001) substrate, and the [11$\bar{2}$0] of the disilicide is oriented along the perpendicular ⟨110⟩ axis [1]. Nanowire growth is attributed to the fact that the disilicide has a small lattice mismatch ($< 2.0\%$) with the Si(001) substrate along one direction but a large mismatch (about $4 \sim 9\%$) along the perpendicular direction. Therefore, the lattice parameters of the rare earth metal disilicides are of critical importance for the growth of nanowires. Because disilicide nanowire growth takes place at high temperatures (usually 573–873 K) and the coefficients of thermal expansion (CTEs) of these di-

silicides are significantly different from those of the Si substrate, the CTEs of these disilicides must be determined in order to have a better understanding of disilicide nanowire growth. However, most of the CTEs of these disilicides are not available. As a part of our on-going research on the phase stabilities of rare earth metal disilicides and the growth of these disilicide nanowires [6–8, 13–16], the CTEs of Sm, Gd, Tb, Dy, Ho, Er, Sc and Er_xGd_{1-x} ($x = 0.45$ or 0.67) hexagonal disilicides were measured. With these CTEs, the lattice parameters of a ternary disilicide $(Er_xGd_{1-x})Si_{1.67}$, for example, can be optimized for nanowire growth by adjusting the composition.

2 Experimental

Samples of these disilicides were prepared by arc melting high purity elements (99.999% Si and 99.9% RE metals, including Sm, Gd, Tb, Dy, Ho, Er, and Sc) in the appropriate ratio of 1 mole metal to 1.67 moles Si. Arc melting was carried out in an atmosphere of high purity argon of 99.998% at a base pressure of 40 mTorr. The arc-melted disilicide ingots were turned over and melted three additional times in order to promote intermixing. Only samples with weight loss during the course of arc melting less than 1% were accepted for further HTXRD study. Each of the ingots was subsequently wrapped with a tantalum foil, contained in a quartz capsule that was evacuated and filled with Ti-deoxidized UHP argon, annealed at 973 K for 12 days to allow the alloy to reach equilibrium, and then quenched in an ice-water bath. The HTXRD data were collected on a PANalytical MPS X-Pert PRO $\theta - \theta$ diffractometer equipped with an Anton–Paar XRK-900 high-temperature stage. The diffractometer was configured with an incident parabolic mirror and diffraction side 0.09° radial divergence limiting slits to achieve parallel beam optics. This configuration effectively removed any diffraction peak shifts resulting from the inherent displacement of the specimen surface due to thermal expansion. Data were collected in a continuous scan mode using Cu K_α radiation with a step size of 0.02° 2θ and a count time of 1 s/step between 20 and 90°. The experiments were carried out in flowing He gas and data were collected at the temperatures listed in Table 1. The specimens were spun continuously to improve the counting statistics. Peak positions and refined

✉ Fax: 608-262-0389, E-mail: chang@engr.wisc.edu

	Disilicides	Temp. (K)	a (Å)	c (Å)
This study	ErSi$_{1.67}$	298	3.7971(2)	4.0874(4)
		473	3.8029(2)	4.0953(4)
		873	3.8249(4)	4.1161(6)
	HoSi$_{1.67}$	298	3.8081(2)	4.1043(4)
		573	3.8209(2)	4.1177(4)
		873	3.8429(2)	4.1339(4)
	DySi$_{1.67}$	298	3.8222(4)	4.1234(4)
		473	3.8304(4)	4.1323(6)
		873	3.8580(6)	4.1519(8)
	TbSi$_{1.67}$	298	3.8426(4)	4.1412(4)
		573	3.8537(4)	4.1558(4)
		873	3.8796(4)	4.1720(4)
	GdSi$_{1.67}$	298	3.8725(4)	4.1722(4)
		673	3.8878(4)	4.2013(4)
		873	3.9081(4)	4.2081(6)
	SmSi$_{1.67}$	298	3.9030(4)	4.2155(6)
		573	3.9120(4)	4.2348(4)
		873	3.9476(6)	4.2486(8)
	ScSi$_{1.67}$	298	3.6587(10)	3.8740(14)
		573	3.6710(10)	3.8876(14)
		873	3.6871(10)	3.9034(16)
	Er$_{0.45}$Gd$_{0.55}$Si$_{1.67}$	298	3.8398(2)	4.1412(4)
		473	3.8468(2)	4.1510(4)
		873	3.8731(4)	4.1697(4)
	Er$_{0.67}$Gd$_{0.33}$Si$_{1.67}$	298	3.8218(2)	4.1178(4)
		473	3.8286(2)	4.1266(2)
		873	3.852(4)	4.149(4)
[19]	ErSi$_{1.67}$	298	3.8006(24)	4.0856(8)
[18]	ErSi$_2$	298	3.785	4.080
		763	3.803	4.099
		863	3.809	4.103
		1253	3.849	4.109
		1343	3.859	4.115
		1473	3.874	4.120
	YSi$_2$	298	3.843	4.143
		473	3.850	4.147
		723	3.854	4.156
		853	3.859	4.160
		1053	3.863	4.165
		1218	3.867	4.170
		1393	3.870	4.171

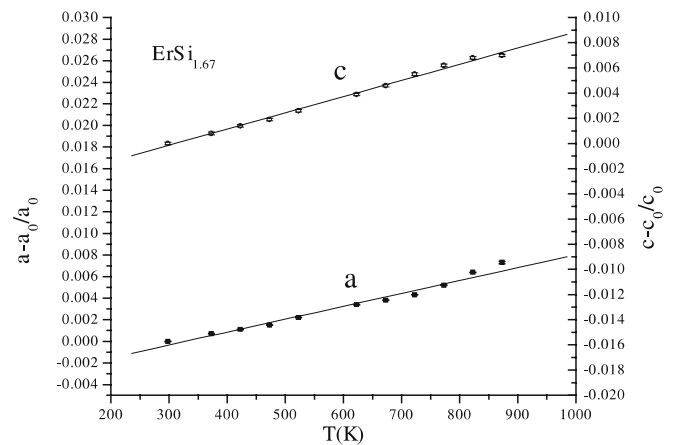**TABLE 1**   Variation of lattice parameters vs. temperature of AlB$_2$ type disilicides

lattice parameters were obtained using the ProFit software package.

3   Data analysis and discussion

The crystal structures of RE silicides are the same as those of AlB$_2$ (C32, hp3), yet the composition is close to 62.5 mol % Si, RESi$_{1.67}$, due to vacancies in the Si sublattice [16]; therefore, these silicides are often referred to as disilicides. The lattice parameters of these disilicides at different temperatures are listed in Table 1. The results reported here are related only to measurements in which a significant change in the lattice parameter occurred. In most of the HTXRD data, extra tiny peaks began to appear at around 600 °C, which are probably due to the oxidation of the powder samples. Significant extra peaks corresponding to ScSi and Si were observed in the Sc disilicide sample even at room temperature consistent with the fact that ScSi$_{1.67}$ is a metastable phase at room temperature and tends to decompose to ScSi and Si [17]. As a reference, the data of ErSi$_2$ and YSi$_2$ meas-

ured by Mayer and Felner [18] are also shown in Table 1. The difference in the lattice parameters of Er disilicide between this study and Mayer's may be due to the compositional difference of the samples, since Er disilicide has a homogeneity range of about 1 at. % [19]. The lattice parameter dependence on composition explains why the lattice parameters of ErSi$_2$ at room temperature measured by Mayer and Felner are different from that of ErSi$_{1.67}$ in this study. The latter agrees well with the lattice parameter values of ErSi$_{1.67}$ obtained by Luzan et al. [19], also shown in Table 1. A typical example of the variation of the lattice parameters vs. temperature is given in Fig. 1. To obtain an average thermal expansion coefficient over the temperature range between 298 K and 873 K, a straight line, constrained to equal zero expansion at 298 K, was fitted to the data. Using this method, the CTEs of the disilicides investigated were obtained and are shown in Table 2, where α_a is the coefficient along the a axis and α_c is that along the c axis. The average linear expansion coefficients, ($\alpha = 1/3(2\alpha_a + \alpha_c)$) are also given in Table 2. The CTEs of most disilicides are more than three times those of the Si substrate, which is about 4×10^{-6} K^{-1} at 873 K [20].

The disilicides measured in this study provide a wide range of lattice mismatch with respect to the Si substrate, ranging from negative mismatch (tension on disilicides) to positive mismatch (compression on disilicides). Since these rare earth metals have similar atomic size, electronegativity and valency and their disilicides have identical crystal structure, according to the Hume–Rothery empirical rules, they may form solid solutions in $(R_xR'_{1-x})Si_{1.67}$ ternaries with R

FIGURE 1   The variation of $(a-a_0)/a_0$ and $(c-c_0)/c_0$ of ErSi$_{1.67}$ vs. temperature, where a_0 and c_0 are the lattice parameters at 298 K along a and c axes, respectively

Disilicides	$\alpha_a \times 10^{-6}$ K^{-1}	$\alpha_c \times 10^{-6}$ K^{-1}	$\alpha_{ave} \times 10^{-6}$ K^{-1}
ErSi$_{1.67}$	12.3±0.6	13.0±0.3	12.5±0.2
GdSi$_{1.67}$	15.3±3.9	15.4±2.7	15.3±2.8
DySi$_{1.67}$	16.7±1.5	11.6±0.2	15.0±1.0
TbSi$_{1.67}$	16.8±3.0	12.9±0.1	15.5±2.0
HoSi$_{1.67}$	15.9±2.0	12.5±0.3	14.8±1.3
SmSi$_{1.67}$	20.0±6.0	13.7±0.2	17.9±4.0
ScSi$_{1.67}$	13.6±0.7	13.2±0.3	13.5±0.5

TABLE 2   Linear thermal expansion coefficients in the temperature range between 298 and 873 K for disilicides

denoting one rare earth metal and R′ another rare earth metal. To verify this idea, two ternary alloys with different composition, $(Er_{0.67}Gd_{0.33})Si_{1.67}$ and $(Er_{0.45}Gd_{0.55})Si_{1.67}$ were prepared and their lattice parameters at different elevated temperatures were also measured. These are shown in Fig. 2. Within the uncertainties of the measured data, both the *a* and *c* lattice parameters of the ternary silicides vary linearly with composition, i.e., following Vegard's law. This indicates that a continuous solid solution of $(Er_xGd_{1-x})Si_{1.67}$ does exist, which suggests that any *a* lattice parameter values between those of $ErSi_{1.67}$ and $GdSi_{1.67}$ can be obtained by adjusting the relative concentrations of Er and Gd. This linear relationship was also observed at high temperatures, as shown in Fig. 2, and thus we can predict the lattice parameter values of a ternary disilicide at high temperature from the CTEs of its corresponding binary disilicides. This rule is expected to hold for other rare earth metals investigated, since they are located either close to or in between Er and Gd in the periodic table.

Therefore, from Fig. 2, we can engineer a ternary disilicide with an *a* lattice parameter perfectly matching the Si substrate in the nanowire length direction at the nanowire growth temperature. With this ternary disilicide, the crystal quality of the nanowire, which is important for the low-dimensional effect, is expected to be significantly improved due to minimized defects. In addition, from Fig. 2, by adjusting the composition, ternary silicides with different *c* lattice parameters at growth temperature can be engineered to obtain nanowires with different widths.

The growth behavior of rare earth metal disilicide nanowires is an interesting phenomenon under study. Pradhan et al. have developed a theoretical model [11] to show the equilibrium shape of a nanowire under anisotropic strain, which arises from the lattice mismatch difference between the width and length directions of the nanowire. If the CTEs are not considered, conclusions significantly differing from the experimental observations would be drawn from this model. In the model, the strain anisotropy is defined as $\delta = 1 - |\varepsilon_W/\varepsilon_L|$, where ε_W and ε_L are the strains of a nanowire in the width and the length directions, respectively and $0 \le \delta \le 1$. The strains of nanowires at different temperatures can be determined with the measured lattice parameters of the disilicides

in Table 1 and the CTE of the Si substrate. The most important argument of this theoretical analysis is that a larger δ will give rise to a larger aspect ratio of a nanowire, i.e., a longer and narrower nanowire. At room temperature, ε_W and ε_L of $ScSi_{1.67}$ are -4.96% and 0.88%, respectively, which results in a δ of 0.81 and ε_W and ε_L of $ErSi_{1.67}$ are 6.05% and -1.13% respectively, which results in a δ of 0.82. The similar anisotropic strains of these two disilicides would lead to similar aspect ratios of these two disilicide nanowires, which is obviously contradicted by the experimental observations that the $ScSi_{1.67}$ nanowires are usually much shorter and wider than the $ErSi_{1.67}$ nanowires [6]. It should be noted that the nanowire growth temperature is about 873 K and thus the CTEs of these two disilicides should be taken into account in the above analysis. At 873 K, however, ε_W of $ScSi_{1.67}$ and $ErSi_{1.67}$ become -4.4% and 6.48%, respectively, and ε_L of $ScSi_{1.67}$ and $ErSi_{1.67}$ become 1.38% and -0.64%, respectively. Therefore, the strain anisotropies, δ, of $ScSi_{1.67}$ and $ErSi_{1.67}$ at the nanowire growth temperature are actually 0.68 and 0.90, respectively. The much lower strain anisotropy of $ScSi_{1.67}$ at the nanowire growth temperature accounts for the experimental observation that the $ScSi_{1.67}$ nanowires are shorter and wider, which can only be correctly understood by considering the CTE.
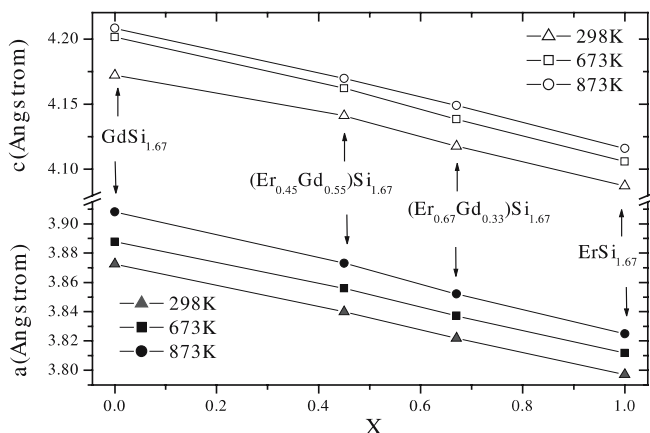
4   Summary

The CTEs of Sm, Gd, Tb, Dy, Ho, Er, and Sc hexagonal disilicides were investigated from RT to the nanowire growth temperature. With the data of these binary disilicides, the CTEs of the corresponding ternary disilicides can be estimated using Vegard's law. Ternary disilicides with optimal lattice parameters at nanowire growth temperature can be engineered to obtain high-quality nanowires. It has also been shown that the CTEs of the disilicides are essential for the correct understanding of nanowire morphology.

FIGURE 2   Lattice parameters of the silicide $(Er_xGd_{1-x})Si_{1.67}$ at different temperatures

REFERENCES

1 Y. Chen, D.A.A. Ohlberg, G. Medeiros-Ribeiro, Y.A. Chang, R.S. Williams: Appl. Phys. Lett. **76**, 4004 (2000)
2 D. Lee, S. Kim: Appl. Phys. Lett. **82**, 2619 (2003)
3 B.Z. Liu, J. Nogami: J. Appl. Phys. **93**, 593 (2003)
4 C. Ohbuchi, J. Nogami: Phys. Rev. B **66**, 16 532 (2002)
5 J.L. McChesney, A. Kirakosian, J.L. Lin, F.J. Himpsel: Nanotechnology **13**, 545 (2002)
6 Y. Chen, D.A.A. Ohlberg, R.S. Williams: J. Appl. Phys. **91**, 3213 (2002)
7 R. Ragan, Y. Chen, D.A.A. Ohlberg, G. Medeiros-Ribeiro, R.S. Williams: J. Cryst. Growth. **251**, 657 (2003)
8 R. Ragan, Y. Chen, D.A.A. Ohlberg, R.S. Williams, J. Yang, Y.A. Chang: IEEE-NANO 2003 **2**, 208 (2003)
9 C. Preinesberger, S.K. Becker, S. Vandré, T. Kalka, M. Dähne: J. Appl. Phys. **91**, 1695 (2002)
10 J. Nogami, B.Z. Liu, M.V. Katkov, C. Ohbuchi, N.O. Birge: Phys. Rev. B **63**, 233 305 (2001)
11 A. Pradhan, N.-Y. Ma, F. Liu: Phys. Rev. B **70**, 193 405 (2004)

12 V.B. Shenoy: Appl. Phys. Lett. **85**, 2376 (2004)
13 Y. Chen, D.A.A. Ohlberg, R.S. Williams: Mat. Sci. Eng. B **87**, 222 (2001)
14 Y. Chen, D.A.A. Ohlberg, G. Medeiros-Ribeiro, Y.A. Chang, R.S. Williams: Appl. Phys. A **75**, 353 (2002)
15 M.L. Huang, J.H. Yang, Y.A. Chang, R. Ragan, Y. Chen, D.A.A. Ohlberg, R.S. Williams: Appl. Phys. A **78**, 1 (2004)
16 C.-X. Ji, M. Huang, J.-H. Yang, Y.A. Chang, R. Ragan, Y. Chen, D.A.A. Ohlberg R.S. Williams: Appl. Phys. A **78**, 287 (2004)
17 P.S. Martsenyuk: Sov. Powder Metall. **27**, 967 (1988)
18 I. Mayer, I. Felner: J. Less-Common Met. **29**, 25 (1972)
19 S.P. Luzan, V.E. Listovnichii, Y.I. Buyanov, P.S. Martenyuk: J. Alloys Compd. **239**, 77 (1996)
20 A.P. Zhemov: Low Temp. Phys. **26**, 908 (2000)